

Twin model for orthorhombic perovskites

Bas B. van Aken, Auke Meetsma, and Thomas T. M. Palstra*
Solid State Chemistry Laboratory, Materials Science Center, University of
Groningen, Nijenborgh 4, 9747 AG Groningen, the Netherlands
(October 29, 2018)

We present a detailed single crystal x-ray diffraction study of twinned orthorhombic perovskites. The diffraction pattern can be indexed on a $2a_p \times 2a_p \times 2a_p$ lattice, but does not obey cubic symmetry relations. The data can be modelled in space group $Pnma$ with a twin based on a distribution of the b axis over three perpendicular cubic axes. This model allows full structure determination in the presence of up to six twin fractions from single crystal x-ray diffraction data.

I. INTRODUCTION

Transition metal oxides with the perovskite structure exhibit a large variety of interesting physical phenomena, including high T_c superconductivity, ferroelectricity, colossal magnetoresistance, and a variety of spin, charge, and orbital orderings. Doping can change the magnetic and electronic properties, which can be reflected in the details of the crystal structure. We are particularly interested in the structural response of phenomena of electronic origin, like Jahn-Teller distortions or orbital order.

Since the metal-oxygen bond lengths and angles determine the exchange interactions, a thorough knowledge of the structure is necessary to understand the physics behind these phenomena. Typically crystal structure information is generated by neutron powder diffraction (NPD). NPD gives direct information about the distances of lattice planes and is very accurate in determining the changes of the lattice parameters with temperature and pressure. Using a full pattern Rietveld Analysis the atomic positions can be determined with an accuracy of 10^{-4} - 10^{-3} .

The alternative is single crystal X-ray diffraction (SXD). SXD is a very powerful experimental application to study the crystal structure of a large variety of materials. In contrast with powder diffraction, which maps all crystal planes to one dimension (d spacing, or angle 2θ), SXD observes all crystal plane reflections separately, even if they are related by symmetry. The relative coordinates of the atoms in the unit cell can be determined from the intensity distribution with the same accuracy as NPD. The major difference is that NPD is sensitive to the nucleus, while SXD measures the electron density, which is of interest to understand the electronic properties.

However, for many perovskites SXD is not used because of unconventional twinning of the crystals. Twinning can complicate the structure determination by creating extra reflection spots and/or superimposing reflections on top of each other. Twinning of the perovskites is complex as the cubic parent structure allows not only simple twin axis and planes, but also 3D twin relations. In this paper we will show a method to analyse twinned single crystals. Moreover, this twin model allows a full structure determination including detailed information

on distortions of both structural and electronic origin. Besides, we also show that one does not need a larger data set, as is usual in the case of twinning.

Using SXD, we observe a $2a_p \times 2a_p \times 2a_p$ unit cell. It is commonly accepted that the unit cell is $\sqrt{2}a_p \times 2a_p \times \sqrt{2}a_p$. The observed unit cell originates from a three-dimensional type of twinning that is not restricted to manganites. The model is most likely of general application for a large variety of perovskite $Pnma$ crystals. This twinning is unique and it involves a distribution of the b axis over three perpendicular cubic axes.

II. THE TWIN STRUCTURE FOR MANGANITES

The manganites have generated considerable attention because of the colossal magnetoresistance effect. The role of magnetic order has been widely discussed as the double exchange, inducing the ferromagnetic order, is required to generate a metallic ground state. The role of orbital order is much less understood. While *local* Jahn-Teller distortions are crucial in explaining the localization of the charge carriers in the paramagnetic state, the *long range* Jahn-Teller ordering is not well studied, except for undoped LaMnO_3 . We will show that the destruction of long range orbital order is a second prerequisite for the metallic ground state. In fact, we will show in a separate paper that with increasing hole doping of LaMnO_3 not the exceeding of a critical concentration but the suppression of the orbital order generates the metallic ground state. The orbital ordering in perovskites with degenerate e_g electrons can be easily measured, whereas for degenerate t_{2g} electrons the Jahn-Teller distortions are much smaller. Furthermore, the $Pnma$ symmetry can accommodate not only the Jahn-Teller ordering, but also a 3D rotation of the octahedra, known as the GdFeO_3 distortion. In this paper we will focus on the main reason why SXD has not been widely used for these perovskites, namely twinning. Twinning in doped LaMnO_3 originates from the transition of the highly symmetric cubic parent structure to the orthorhombic symmetry, that accommodates both the GdFeO_3 and the Jahn-Teller distortion. In thin films *ac* twinning has been observed. The solution of the twin relations in the crystals allow us to study in

detail the ordering of these compounds as influenced by temperature, magnetic state and doping concentration. In this paper we will focus on the twin relations.

At high temperatures most AMnO_3 are cubic with a unit cell of $a = 3.9 \text{ \AA}$. Due to both the small average A-site radius and the JT effect the MnO_6 octahedra are rotated and distorted at lower temperatures. We will show that our crystals are twinned. We present here an accurate description of the origin of the twinning, the detwinning process and show that we can still determine the temperature dependence of the structure by measuring only the reflections of the main fraction in one octant of the hkl space.

Twinning is reported before in AMnO_3 perovskites and related structures. For instance, neutron powder experiments on LaMnO_3 showed reflections, at temperatures above the Jahn-Teller transition, that could be indexed on a double cubic unit cell. But full pattern refinement was only possible in the orthorhombic space group $Pnma$.¹ Single-crystal electron diffraction showed a double cubic unit cell for SrSnO_3 , even though CaSnO_3 is orthorhombic.² Electron microscopy, however, showed the existence of coherent domains, with perpendicular orientations of the doubled b axis. The structure was deduced via the O’Keefe-Hyde relations.³

The single crystal was mounted on an ENRAF-NONIUS CAD4 single crystal diffractometer. The temperature of the crystal was controlled by, heating, a constant nitrogen flow. Initial measurements were done at 180 K. Temperature dependent measurements were performed on a diffractometer with an adjustable temperature set-up, between 130 K and 300 K.

III. CRYSTAL STRUCTURE

Most structure research of perovskites focuses on the Mn-O distances and the Mn-O-Mn angles, as these parameters determine the super- and double exchange interactions. Here, we like to stress the importance of a complete structure refinement, including the La-position and the rotation/distortion of the MnO_6 octahedra. The basic deformations that determine the deviation from the cubic structure are the GdFeO_3 distortion and the Jahn-Teller distortion.

The basic building block of the perovskite structure is a 3.9 \AA cube with Mn in the centre and O at the face-centers. The oxygen ions co-ordinate the Mn to form MnO_6 octahedra. The A atoms are located at the corners of the cube. The undistorted ‘parent’ cubic structure rarely exists, but distorts conventionally to an orthorhombic or rhombohedral symmetry. For an ideal perovskite the ratio between the radii of the A site ion and the transition metal ion is such that the tolerance factor

$$t = \frac{\langle r_{A^{2/3+}} \rangle + r_{O^{2-}}}{\sqrt{2}(\langle r_{Mn^{4/3+}} \rangle + r_{O^{2-}})} \quad (1)$$

is equal to one. In the La-Ca system the tolerance factor varies from 0.943 to 0.903 going from LaMnO_3 to CaMnO_3 .

A. GdFeO_3 rotation

Due to the small radius of the A-site ion, with respect to its surrounding cage, the MnO_6 octahedra tilt and buckle to accommodate the lanthanide. This is known as the GdFeO_3 distortion. The cubic state allows one unique oxygen position. Due to the GdFeO_3 distortion we need two inequivalent positions to describe the structure. O1 is the in-plane oxygen, on a general position, x, y, z . Two opposite Mn-O1 bonds have the same length, but the perpendicular bonds need not to be equal. O2 is the apical oxygen, located on a fourfold $x, \frac{1}{4}, z$ position on the mirror plane. Mn-O2 bonds are always of the same length. Both in the undistorted and the distorted perovskite, the O-Mn-O bond angles are $180^\circ (90^\circ)$, but due to the buckling Mn-O-Mn bond angles are no longer 180° . A pure GdFeO_3 distortion can be obtained with equal Mn-O bond lengths.

B. Jahn-Teller distortion

The Jahn-Teller effect originates from the degenerate Mn d^4 ion. Two, possible, distortions are associated with the Jahn-Teller effect. Q2 is a orthorhombic distortion, with the in-plane bonds differentiating in a long and a short one. Q3 is the tetragonal distortion with the in-plane bond lengths shortening and the out-of-plane bonds extending, or vice versa^{4,5}. The main result of the JT effect, Q2 and Q3, is that the Mn-O distances become different, which lifts the degeneracy of the t_{2g} and e_g levels.

C. Glazer’s view on the octahedra

There are three possible rotations for a rigid MnO_6 octahedron. One, η_y , changes the atomic positions of the O2 atom only. The others have an effect on the atomic positions of both O1 and O2. These movements will also affect the position of the La atom⁶. Glazer⁷ identified all possible sequences of rotations for the perovskite system. Two of these sequences create the symmetry elements that make up the standard perovskites. In Glazer’s notation: $a^- b^+ a^-$ *) yields orthorhombic $Pnma$ and $a^- a^+ a^-$

*) $p^- q^+ r^0$ means that along $[100]$ a rotation of size p is alternated positive and negative, along $[010]$ a rotation of size q is always (arbitrarily) positive, and along $[001]$ there is no rotation.

will result in rhombohedral $R\bar{3}c$. As Glazer worked in a pseudocubic $2a_p \times 2a_p \times 2a_p$ system we have to translate these rotations to the orthorhombic unit cell, which gives a^-b^+0 . This means that the rotation around the c axis, η_z , is zero. This is in agreement with the observation that the four positions of O2 near the Mn at 0,0,0 have the same distance to the $y = 0$ plane, albeit two are positive and two are negative. By rotating the MnO_6 octahedra around the x axis, two oxygen are raised from their cubic position and two are lowered. Here we neglect the influence of a rotation η_y on these coordinates. As a result of $\eta_z = 0$ the fractional x co-ordinate of O1 is also zero. In practice small deviations are found, indicative of the non-rigid behaviour of the MnO_6 octahedra. Typically in AMnO_3 two rotations and the Q2 JT distortion are observed.

One effect of the GdFeO_3 distortion is that the number of formula units per unit cell is enlarged. The unit cell is doubled in the b direction, with respect to the original cubic cell. The ac plane is also doubled, resulting in $b \approx 2a_p$, and $a \approx c \approx \sqrt{2}a_p$. Despite the rotations and distortion, the structure remains in origin cubic. The shifts of the atoms in the unit cell are small. Furthermore, Mn stays roughly octahedrally surrounded although the Mn-O distances tend to differ and some O-Mn-O angles may be no longer perfectly 90° or 180° . The small deviations from the cubic symmetry are reflected in the intensities of the reflections. To illustrate this point, we transform an arbitrary, cubic, reflection hkl to the orthorhombic setting by $h'k'l' = h+l, 2k, h-l$. Thus orthorhombic reflections with k' even and h' and l' both even or both odd stem from planes that already existed in the original cubic unit cell. We observe in diffraction patterns of orthorhombic perovskites that reflections that originate from cubic crystal planes have higher intensities than those that do not.

IV. TWIN MODEL

Reflections in reciprocal space are experimentally observed at a regular distance in three orthogonal directions, corresponding to a cubic lattice spacing of 7.8 \AA in real space. Although the three orthonormal axes have equal lengths, we could not observe the threefold rotation axis along $\langle 111 \rangle$, required for cubic symmetry. However, studying the intensity distribution of planes in hkl space with constant h , k or l showed much regularity as is shown in Fig. 1. We propose a twinned structure consisting of coherent $Pnma$ domains. Due to partial overlap this results in a metric cubic system with $a \approx 2a_p \approx 7.8 \text{ \AA}$.

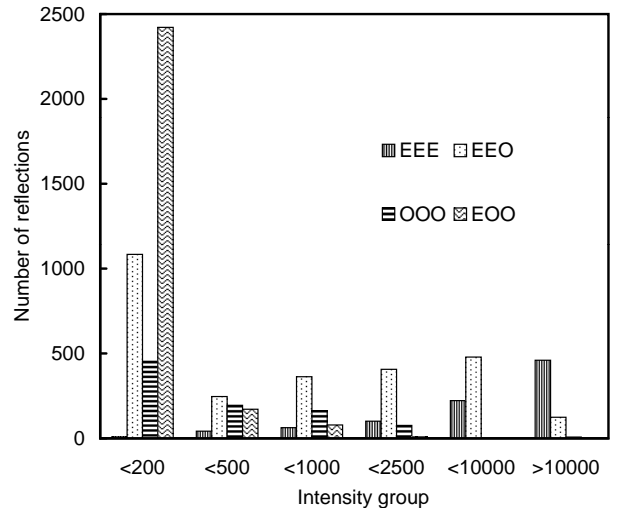


FIG. 1. The number of reflections of the different types versus intensity ranges. Low intensities, $I < 200$ are mostly EEO, while high intensities, $I > 2500$, are of the types EEE and EEO.

Twinning is often observed in crystals with a reduced symmetry. For instance, the orthorhombic perovskite LaMnO_3 has lower symmetry than cubic SrTiO_3 . Conventional twin models keep one characteristic axis unchanged and form the domains by rotation around that axis. This is commonly observed in constrained epitaxial thin films and pseudo-two-dimensional crystals like $\text{YBa}_2\text{Cu}_3\text{O}_{7-\delta}$. Another standard twin is inversion twinning, found in non-centrosymmetric systems. Due to the inversion twin, pseudo-centrosymmetry is obtained or a net polarisation in ferroelectric compounds is reduced to zero.^{8,9} Both twin models have usually the property that either all twin domains have reflections that lie on top of each other, merohedral twins, or there is a non-commensurate set of reflections, *e.g.* in monoclinic unit cells. Here we propose a more extensive form of twinning, where the different reflections of different domains partially coincide, giving rise to the observed metrically cubic system.

The transformation of cubic to orthorhombic symmetry requires a designation of a , b , and c with respect to the degenerate cubic axes. There are three possibilities to position the doubled b axis along the three original cubic axes. Thus we propose that the three fractions' b axes are oriented along the three original axes of the cubic unit cell, as sketched in Fig. 2. This twin model consists of a $Pnma$ unit cell, transformed by rotation along the 'cubic' $[111]$ axis. We still have the freedom to choose the a and c axes, perpendicular to the b axis, and rotated 45° with respect to the cubic axes. Therefore, this model yields six different orientations of the orthorhombic unit cell. As the differences between $a/\sqrt{2}$, $b/2$ and $c/\sqrt{2}$ are small, we observe the reciprocal superposition of the six orientations as metrically cubic.

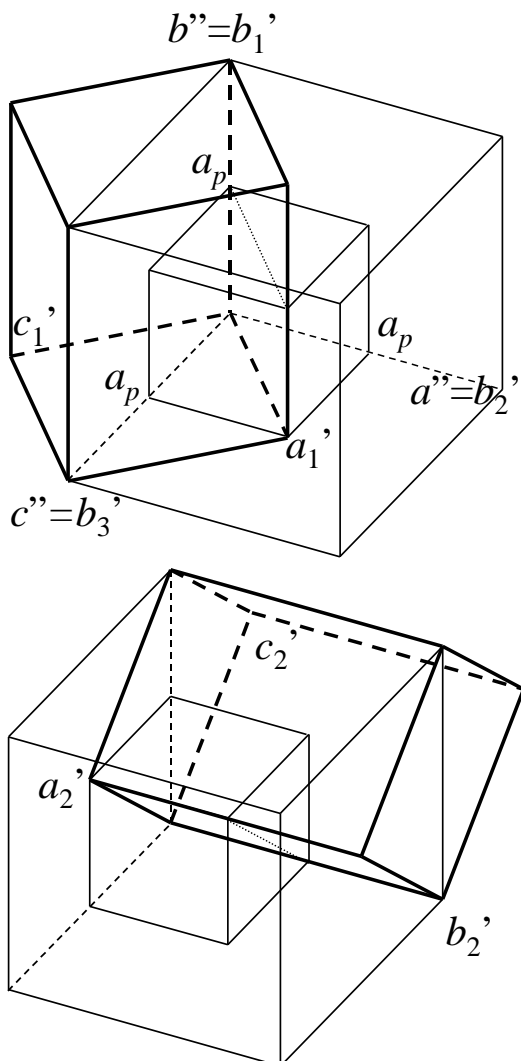


FIG. 2. Two of three possible orientations of the $Pnma$ unit cell in the observed $2a_p \times 2a_p \times 2a_p$ ($a'' \times b'' \times c''$) unit cell. b_1' , b_2' and b_3' denote the orientations of the doubled axes along the original cubic axes, a_p . Note that the choice of a' and c' is still open, after choosing an orientation for the b' axis.

The standard refining programs can work with twin models, but only if they consists of merohedral twins. In our case, the reflections do not correspond with an orthorhombic unit cell, but with a, twice as large, cubic unit cell. In appendices A and B, we will elaborately explain the transformation from orthorhombic to double cubic and the way we worked around the refining program.

We first measured a hemisphere in hkl space with $-20 < h < 20$, $-20 < k < 20$, and $0 < l < 20$. On this dataset, we could refine our twin model with the six fractions, including the Ca concentration on the A site. Measuring a large range in hkl space requires a large amount of time, roughly 10 days in the present set-up. Conventionally, for crystals with orthorhombic unit cells measuring one octant is sufficient. From refinements on selected parts of the dataset, we concluded that we could investigate the

structure at different temperatures by only measuring the positive octant of the main fraction, thereby limiting the measuring time considerably.

V. DISCUSSION

The observed reflections could be indexed on a cubic lattice with $a \approx 7.8$ Å. Although the three axes had equal lengths, we could not observe the required threefold symmetry axis along $\langle 111 \rangle$ for cubic symmetry. This is shown for EEO reflections in Fig. 3. Furthermore, studying the intensity distribution of hkl planes with constant h , k or l showed much regularity, as is shown in appendix A. Rodríguez-Carvajal *et al.* noted that their neutron powder spectra of pure LaMnO_3 could be indexed in a cubic $2a_p \times 2a_p \times 2a_p$ unit cell, above the Jahn-Teller transition temperature.¹ They did not observe a splitting of the peaks. Nevertheless, they could not refine the structure in a cubic unit cell. Note that in powder diffraction spectra there is no direct method to observe the threefold symmetry along the body diagonal. The refinement of the spectra has been done in the conventional $Pnma$ setting. They suggested that the powder is twinned but could not give evidence for that, as they only studied powders. The observed reflections, the systematic extinctions and the non-cubic intensity distribution suggest

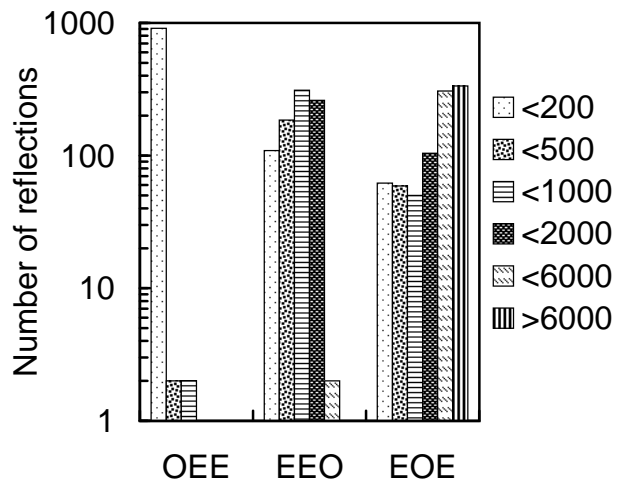


FIG. 3. The number of reflections versus the types OEE, EEO and EOE for different intensity ranges. OEE, b' parallel to a'' , has mostly very low intensity. Reflections EOE, b' parallel to b'' , have a broad range of intensities. In cubic symmetry, these distributions should be identical for absorption corrected data, which we considered.

Typically, Ca-doped LaMnO_3 has space group $Pnma$. We propose a twinned structure consisting of coherent $Pnma$ domains, which results in a metric cubic system with $a \approx 7.8$ Å. The model is identical to the twinning observed by electron microscopy in CaSnO_3 .² They could however not refine their $2a_p \times 2a_p \times 2a_p$ data on dif-

ferent $Pnma$ domains, and deduced the structure from phenomenological relations³ and the similarities with $SrSnO_3$. In the present work, the different contributions of the twin fractions to the total integrated peak intensity are taken into account. The refined model consisted of the regular parameters in single crystal diffractometer. We considered for each observed reflection the related orthorhombic reflections for the applicable twin fractions and used an identical unit cell. This way, we can refine both the atomic positions of the asymmetric unit and the volume ratio of the twin domains simultaneously.

Several crystals were measured and refined with this detwin model. The refinements showed that for every crystal the distribution of the volume over the twin fractions is different. This is an indication that our crystals are really twinned. Other structural deformations would lead to a constant, not sample dependent, effect on the structure factors and therefore to the same fractions of the twin domains. We can also conclude that the size of the twin domains must be slightly smaller than the magnitude of the measured crystals, i.e. several tenths of a millimeter. Larger twin domains would give rise to crystals of one single domain and smaller domains are more likely to produce a constant spreading of the domains. Non-regular, though constant, distributions could signal a preferential growth direction of the crystal.

A. Intensity distribution

Careful analysis of the intensity distribution showed extra evidence for the proposed models. The full dataset shows that reflections hkl of type EEE^\dagger are by far the strongest. Reflections having one odd Miller index, OEE, EOE, EEO, are second in intensity. EOE has the highest intensity of these reflections as seen in Fig. 3. To understand the intensity distribution in the $2a_p \times 2a_p \times 2a_p$ unit cell, we examine the structural deformations. Despite the effect of Jahn-Teller distortions, $GdFeO_3$ rotations and twinning, the structure remains in origin cubic. This means that the intensity distribution of the peaks with high intensity will always mimic the intensity distribution of the peaks of the undistorted cubic perovskite. An arbitrary reflection, in the cubic unit cell, hkl , is transformed to the orthorhombic unit cell as $h+l$, $2k$, $h-l$. Thus orthorhombic reflections with h' and l' both even or both odd and k' even stem from the original cubic unit cell. Although the fact that the $h'k'l'$ =EOE reflections do not originate from the original cubic planes, they are allowed in the $Pnma$ symmetry. Reflections $h'k'l'$ that satisfy these conditions have higher intensities than those that do not.

[†]E denotes an even value for the Miller indices, O stands for odd

To double the $Pnma$ unit cell to a $2a_p \times 2a_p \times 2a_p$ unit cell, a reflection $h'k'l'$ is transformed to $h''k''l''$ as $h'+l'$, k' , $h'-l'$. Please note that we do not explicitly mention the different orientations of the orthorhombic unit cell. If the regarded b axis is not parallel with k'' , then the indices should be cycled appropriately. The transformation yields that double cubic reflections with $k'' = k' = 2n$ originate from single cubic reflections, with $k = n$. However, $k'' = 2n + 1$ reflections originate from single cubic non-integer indices k , and will therefore have less intensity. This explains why the measured $h''k''l''$ =EEE reflections are strongest and EOE are one order of magnitude less strong. We have seen that $h'' = h'+l'$ and $l'' = h'-l'$ thus h'' and l'' are always both even or both odd. Therefore EOE has only contribution of the fractions with k'' corresponding to the orthorhombic b axis. OEE and EEO originate from fractions with their b axis parallel to h'' and l'' , respectively. The fact that our observed EOE is stronger than OEE and EEO, indicates that, by chance, the observed b axis, or k'' direction, is parallel with the b axis or k' direction of the largest twin fraction.

B. Refinement

We determined both the Ca content and the volume fractions of the twins by measuring a full hemisphere of hkl space. We compared the results with a refinement on only one octant of these measured reflections. The outcome was equivalent within the error bars. We refined again fixing the twin fractions and Ca concentration to the values found for the first refinement on the large dataset, and allowing only the atomic co-ordinates and anisotropic displacement parameters (adp's) to change. This resulted in the same structural model as found with the complete structure determination on the largest dataset. We concluded that apparently the refinement with fixed fractions and Ca concentration is insensitive for the size of the dataset. This can be understood if we view the symmetry relations and Friedel pairs. Due to the Patterson symmetry, mmm the relation $F(\bar{h}kl) = F(hkl)$ is valid for all structure factors. Friedel pairs are reflections that have intrinsically the same structure factor, related thus by symmetry and ignoring absorption and anomalous scattering effects. Although we have six different orientations, one octant chosen for a particular orientation will still contain data of all fractions that can be transformed in such a way that every $h'k'l'$ is included for all three b directions.

VI. CONCLUSION

We have shown that crystals of $La_{1-x}Ca_xMnO_3$, with $x = 0.19$, have the orthorhombic $Pnma$ space group, although they appear in single crystal diffractometry metrically cubic. The metric cubic appearance results from

twinning in which the doubled b axis of the $Pnma$ cell is oriented along all three cubic axes of the single cubic unit cell during crystal growth or cooling. This twin model allows successful structure refinements of single crystal x-ray diffraction data.

APPENDIX A: DATA ANALYSIS

Here we describe the effect of the twin model on the visibility of the standard $Pnma$ reflection conditions as well as a detailed analysis of the intensity distribution of a model crystal with $Pnma$ symmetry and of the measured reflections in double cubic setting. The first step in space group determination is to look for systematic absences in the list of reflections. We observe no intensity for the reflections shown in table I. Note that the indices are in double cubic setting and therefore allow cyclic permutation, *i.e.* $h00$, $0k0$ and $00l$ are all represented by $h00$. These reflection conditions allow only the space groups $P2_13$ and $P4_232$. However, these space groups have as reflection condition only $h00 : h = 2n$. This suggests that we have more information than can be attributed to these space groups. Attempts to determine the structure using these space groups were unsuccessful. Furthermore, the observed and, for cubic systems, anomalous, reflection conditions suggested that we might be looking at a twinned crystal. In the next paragraph, we present the transformation of the reflection conditions for orthorhombic $Pnma$ according to the presented twin model.

TABLE I. Extinct reflections as observed in the $2a_p \times 2a_p \times 2a_p$ data set.

Reflection	Extinction condition
$h00$	$h \neq 2n$
$h\bar{h}0$	$h \neq 2n$
hkh	$h \neq 2n, k = 2n$
$hk\bar{h}$	$h \neq 2n, k = 2n$

1. Extinctions

The $Pnma$ reflection condition $0k'0 : k' = 2n$ is transformed to double cubic as $0k''0 : k'' = 2n$ and cyclic permutation. This corresponds to the reflection condition $h''00 : h'' = 2n$ in table I. $Pnma$ reflections of the type $h'0h'$ are transformed to $h''00$, with $h'' = 2h'$. This implies that $h'0h'$ never contributes intensity on reflections $h''00$, with h'' odd. Conversely, if we do not observe intensity on all reflections $h''00 : h'' \neq 2n$, then all of the constituting $Pnma$ reflections should be absent.

To transform and understand the other reflection conditions of $Pnma$ we have to take into account that an orthorhombic, and also a cubic, unit cell implies that hkl is equivalent upon sign reversal of each of the Miller indices. The $Pnma$ reflection condition $h'00 : h' = 2n$ becomes $h''0h'' : h'' = 2n$ and similarly $00l'$ transforms to $l''0\bar{l}''$. But as we just stated, $h''0h''$ is identical to $h''0\bar{h}''$. If we combine reflections then a reflection condition is fulfilled if any of the contributing parts has intensity. To obtain extinction, all contributing reflections should be extinct. As $00l'$ has no extinction condition, *i.e.* intensity for all l' , they will contribute to all $h''0h''/h''0\bar{h}''$ reflections, and the $Pnma$ reflection condition $h'00 : h' = 2n$ is masked.

The overlap of different reflections occurs also for $0k'h'$ and $h'k'0$. These transform to $h''k''\bar{h}''$, and $h''k''h''$. Therefore, we cannot disentangle $0k'h'$ and $h'k'0$ in the measured double cubic cell. The $Pnma$ reflection conditions for $0k'l'$ and $h'k'0$ are $k'+l' = 2n$ and $h' = 2n$, respectively. $h''k''h''$ and $h''k''\bar{h}''$ are found to be extinct for $h'' \neq 2n$ and $k'' = 2n$ in the double cubic setting. To have these reflection extinct, all contributing $Pnma$ reflection conditions must be extinct. This implies that both $h' = 2n$ and $k'+h' = 2n$, the reflection conditions for the contributing $0k'h'$ and $h'k'0$, may not be fulfilled. Thus $h'' \neq 2n$ and this yields $k'' = 2n$.

Now we consider reflections of the type $h''k''h''$ that are not extinct. Our twin model yields six fractions that can contribute to the considered reflections.

1. $h'' = 2n$ and $k'' = 2n$. Reflections EEE have contributions from the four fractions with the doubled b' -axis parallel to either a'' or c'' , this is also true for reflections OOO. In addition, we also have contributions from the two fractions with b' parallel to b'' , *i.e.* from $h'k'0$ and $0k'h'$.
2. $h'' \neq 2n$ and $k'' = 2n$. Reflections OOO, in addition to the four fractions with the doubled b' -axis parallel to either a'' or c'' , have one additional contribution from $0k'h'$. In the special case that $h'' = k''$, for both EEE and OOO, then two of the four fractions, parallel to a and c contribute.
3. $h'' = 2n$ and $k'' \neq 2n$. Reflection EOE, have only a contribution from the $h'k'0$ reflection, with b' parallel to the observed b'' axis.

We have shown that the intensity of observed $h''k''h''$ reflections depend on odd or even. We conclude that $h''k''h''$ reflections are extinct for OEO , while the other reflections have contributions from up to six twin fractions.

2. Intensity in double cubic setting compared with $Pnma$

We can also learn something about the twinned origin by studying the intensity distribution. Our twin model provides a natural explanation for the hierarchy in intensities of the reflections. First, we consider the known transition from the single cubic unit cell to the orthorhombic one to elucidate the patterns that are inherent to perovskites. Then we proceed to show how these patterns are convoluted in the double cubic, twinned model.

The intensity distribution of a normal $Pnma$ perovskite is shown in Fig. 4. In conventional orthorhombic $Pnma$ the reflections $h'k'l'$ with $h'+l' = 2n$ are stronger than $h'+l' \neq 2n$. From these, the $k = 2n$ reflections are stronger than the $k \neq 2n$ ones. This can be attributed to their origin in the 3.9 Å cubic structure. The $h'k'l'$ reflections in orthorhombic setting originate from hkl in the single cubic cell for $h' = h+l$ and $l' = l-h$. Therefore, h' and l' will always be both even or both odd. In other words if $h'-l' \neq 2n$ then the reflections originate from a crystal plane in the single cubic setting with a non-integer Miller index, *i.e.* a superlattice reflection and their intensities are usually weak. The same argument can be applied to k . As $k' = 2k$, thus $k' = 2n$ originate from a regular crystal plane, $k' \neq 2n$ is the superlattice reflection. These $k' \neq 2n$ however appear to have somewhat more intensity than the $h'-l' \neq 2n$ reflections.

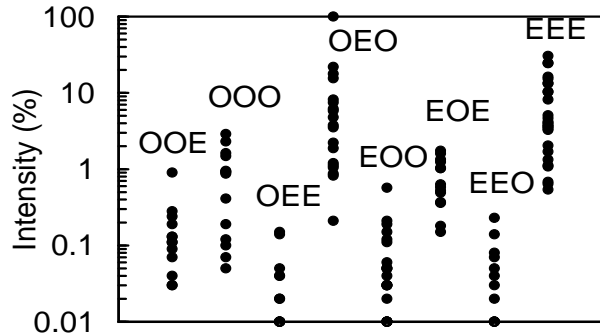


FIG. 4. The calculated intensities for a conventional perovskite, subdivided with respect to odd and even of the Miller indices. $k = 2n$ reflections are strongest, if $h'+l' = 2n$. Reflections with $h'+l' \neq 2n$ have roughly 100 times less intensity.

We observe the following patterns in the intensity distribution in the double cubic cell. First, reflections EEE are generally the strongest, EOO usually absent, or very

weak. If we ignore the allowed permutations in cubic setting, the following hierarchy can be made. EOE reflections were much stronger than EEO, which are again stronger than OEE. Likewise, OEO reflections were, although weak, stronger than OOE and again stronger than EEO.

In conventional $Pnma$ structure we found that if $h'+l' \neq 2n$ than reflections with $k' \neq 2n$ are stronger than those with $k' = 2n$. In our notation, for the $Pnma$ structure this yields (EEE=OEO) \gg (OOO=EOE) \gg (OOE=EEO) $>$ (OEE=EEO). So there are roughly four intensity groups. We can correlate these four groups with the four types of reflections we measured in the supercubic setting, with the following intensity hierarchy: EEE \gg EEO \gg OOO $>$ EEO.

We consider here the transformation from the orthorhombic to the double cubic setting for the in-plane indices, h' and l' . Double cubic indices are calculated with $h'+l'$ and $h'-l'$, therefore h'' and l'' will be both even or both odd. Reflections of the type $E?O$ or $O?E$ will have no intensity of the twin with b' parallel to b'' , as they are not originating from an 'integer' crystal plane. But we have a mixing of different orientations of the b' axis along the three cubic axes a'' , b'' and c'' . We can cycle the indices of these reflections such that we get either $E?E$ or $O?O$, and from the corresponding twin, b' parallel to a'' or c'' we do have intensity on these reflections. EOE and OEO will only have contributions from this particular setting. EEE and OOO can be cycled and in general have contributions from all six orientations.

3. distribution of the twins

If we consider that the main part of the intensity in the double cubic setting originates from the largest twin fraction, we can search for the orientation of the largest fraction. That b' axis is expected to be oriented along one of the measured double cubic axis. We can not differentiate the two fractions with parallel b' and perpendicular a' and c' . We considered groups of reflections with cycled indices, having either one odd, OEE, or one even index, EEO. Roughly, the intensities of the reflections within these groups occurred with ratio 70:20:10. This suggested that one twin had 70% of the volume, the others 20% and 10%. Now we sorted these reflections to find the corresponding orientations. The sort parameter is the observed double cubic axis that corresponded with the odd indices in OEE, and vice versa. Only cycled reflections that occurred three times with measurable intensity were taking into account. We found that $I_{a''} : I_{b''} : I_{c''} = 5 : 80 : 15$. The constraint that all three intensities have positive values, ignores the weakest reflections. It also ignores Bijvoet pairs, as we only measured $-20 < l'' < 2$. If we indeed had a cubic system then these variations should be zero within standard deviation. The distribution of the intensities with respect to the different axis, strongly suggests that the crystal is

twinned.

APPENDIX B: IMPLEMENTATION IN REFINEMENT

Here we describe the model and the application by SHELXL. The standard refining programs can work with merohedral twin models. However, in our case, the reflections do not coincide with one orthorhombic unit cell. Every observed reflection has contributions of up to six twin fractions. We measured both in the double cubic setting as in the orthorhombic setting of the main twin fraction. We transformed the $h''k''l''$ indices to the six possible twin orientations. Three of the possibilities are given by

$$h'k'l' = \frac{1}{2}(h'' + l''), k'', \frac{1}{2}(h'' - l'') \quad (\text{B1})$$

$$h'k'l' = \frac{1}{2}(l'' + k''), h'', \frac{1}{2}(l'' - k'') \quad (\text{B2})$$

$$h'k'l' = \frac{1}{2}(k'' + h''), l'', \frac{1}{2}(k'' - h'') \quad (\text{B3})$$

The other three can be acquired by changing h' for l' and l' for $-h'$.

A new software program TWINSXL was developed to transform the standard data file, HKLS, by using the appropriate transformation matrices from a second input file.¹⁰ The new data file constitutes of lines of h, k, l , intensity plus standard deviation and twin fraction number. We used the "HKLF 5" option of SHELXL to refine data. The refinement uses a crystal model for the orthorhombic structure with the normal, adjustable variables. Five variables for the twin fractions were added, the sixth fraction is calculated as the complement of the other five fractions. The sum of the appropriate calculated intensities for all fractions was compared with the observed integrated intensities.

⁸ C. Rao and J. Gopalakrishnan, *New directions in solid state chemistry*, 2nd ed. (Cambridge University Press, 1997), page 385.

⁹ B. B. Van Aken, A. Meetsma, and T. T. M. Palstra, *Acta Crystallogr.* **C57**, 230 (2001).

¹⁰ A. Meetsma, TWINSXL, software package, Solid State Chemistry, University of Groningen, 2000.

* Email: Palstra@chem.rug.nl

¹ J. Rodríguez-Carvajal, M. Hennion, F. Moussa, A. H. Moudden, L. Pinsard and A. Revcolevschi, *Phys. Rev. B* **57**, R3189 (1998).

² A. Vegas, M. Vallet-Regí, J. González-Calbet, and M. Alario-Franco, *Acta Crystallogr.* **B42**, 167 (1986).

³ M. O'Keefe and B. G. Hyde, *Acta Crystallogr.* **B33**, 3802 (1977).

⁴ J. Kanamori, *J. Appl. Phys.* **31**, 14S (1960).

⁵ Y. Yamada, O. Hino, S. Nohdo, R. Kanao, T. Inami and S. Katano, *Phys. Rev. Lett.* **77**, 904 (1996).

⁶ T. Mizokawa, D. I. Khomskii, and G. A. Sawatzky, *Phys. Rev. B* **60**, 7309 (1999).

⁷ A. M. Glazer, *Acta Crystallogr.* **B28**, 3384 (1972).